Results in Physics 13 (2019) 102303

Contents lists available at ScienceDirect

Results in Physics

journal homepage: www.elsevier.com/locate/rinp

Machining performance of hard-brittle materials by multi-layer micro-nano crystalline diamond coated tools

Guangyu Yan[a], Yuhou Wu[a,*], Daniel Cristea[b], Feng Lu[a], Yibao Wang[c], Dehong Zhao[a], Mircea Tierean[d], Lusheng Liu[c,*]

[a] Faculty of Mechanical Engineering, Shenyang Jianzhu University, 110168 Shenyang, China
[b] Materials Science Department, Transilvania University, 500036 Brasov, Romania
[c] Shenyang National Laboratory for Materials Science, Institute of Metal Research, Chinese Academy of Sciences, 110016 Shenyang, China
[d] Materials Engineering and Welding Department, Transilvania University, 500036 Brasov, Romania

ARTICLE INFO

Keywords:
HFCVD
Diamond coating
Multilayer
Cutting tool
Hard-brittle material

ABSTRACT

Single layer diamond coatings, deposited on cobalt cemented tungsten carbide (WC-Co), with CH_4 concentrations of 1%, 3% and 5% were prepared, by hot filament chemical vapor deposition (HFCVD). Moreover, according to the characteristics of different kinds of diamond structure, observed on the single layer coatings, multi-layer crystalline diamond films with micro-nano structures (composed of the 1% and 5%-type coatings) were prepared. The objective was to cumulate the increased interfacial adhesion and mechanical properties of each single layer diamond coating, into one multilayer coating, capable of resisting the efforts present between a milling tool and a hard-brittle material (natural marble). The coating morphology, structure, and resistance to crack propagation of the diamond films were evaluated. Furthermore, cutting tests with diamond-coated tools were performed, while observing the machining life and wear mechanism, on a hard-brittle material (marble). The results on the single layers showed that with the increase of the concentration of CH_4, the adhesion to the WC-Co substrate, as well as the resistance to crack propagation is decreasing. The multilayer coating structure shows benefits from the single layer coatings, i.e. improved adhesion to the substrate and inhibition of crack propagation, while the tool life and machining stability are significantly better than the single diamond layer coated tools.

Introduction

Hard-brittle materials such as ceramics, marble, and granite, have superior properties such as: high hardness, good wear resistance, high temperature resistance, and stable physical and chemical properties [1]. However, the low machinability of hard-brittle materials such as these requires super-hard machining tools with excellent cutting performance. These technical limitations remain to be a problem in the machining process of complex three-dimensional structures [2].

Some improvements regarding the cutting performance and service life for tungsten carbide cutting tools were reported, mainly by depositing a diamond coating on the carbide tool, usually by chemical vapor deposition (CVD). Consequently, the cutting performance and effective service time of diamond coated tools was reported to be significantly better, compared to the uncoated WC-Co tools [3]. Polini [4] found that the application of smother diamond films can reduce cutting forces by facilitating chip evacuation. However, the impact of high frequency variation of the milling force still poses a problem. As reported by Almeida et al. [5], fractures occur in the diamond film, ultimately leading to coating-substrate spallation, after the machining of EDM graphite. This variation of the milling force is related to the fact that, depending on the cutting tool design, each flank is only momentarily in contact with the workpiece, followed by the next flank, and so on.

The deposition parameters and coating microstructures have a significant impact on the adhesion of the coating to the substrate. Ali et al. [6] concluded that CH_4 concentration has an influence on growth rate, surface roughness and quality of diamond films. Generally, in case of CVD deposited coatings, the gas concentration ratio of CH_4 and H_2 determine the crystal form and grain size of the diamond coating [7]. Significant differences in adhesive strength of MCD (microcrystalline diamond) and NCD (nanocrystalline diamond) coatings were observed. Dumpala et al. [8] found that the MCD samples showed superior adhesion properties, in comparison to NCD samples, through scratch tests.

* Corresponding authors.
E-mail addresses: wuyh@sjzu.edu.cn (Y. Wu), lsliu@imr.ac.cn (L. Liu).

https://doi.org/10.1016/j.rinp.2019.102303
Received 5 March 2019; Received in revised form 28 March 2019; Accepted 17 April 2019
Available online 26 April 2019

Relatively easier delamination was observed in NCD-coated tools in composite machining, as reported by Qin et al. [9]. In order to take advantage of microcrystalline diamond and nanocrystalline diamond films, composite and multilayer diamond films have been proposed. Khomich et al. [10] analyzed the mechanical properties of multilayer diamond films by MP-CVD method and concluded that the coatings display good adhesion and wear resistant properties. Sun et al. [11] obtained a composite diamond film including a layer of MCD film and multilayer of NCD films, with improved cutting performances in the turning process of Al metal matrix composites (15% SiC). The analysis of the machining properties of multi-layer diamond coatings was made through a bias-enhanced HFCVD technique by Wang et al. [12]. The results indicated that multilayer (nano-micro-nano-micro) diamond coated tools (substrate material: WC-6% Co) exhibited longer working life compared to the single coated ones. However, the machining performance and wear characteristics of coated tools were only analyzed as function of the tribological properties, regardless of the residual stress and internal toughness. There are insufficient systematic comparison studies on the mechanical properties and machining properties of diamond coated tools, especially subjected to milling of hard-brittle materials. Therefore, the mechanism of coating characterization in conjunction with machining performances of single layer and multilayer diamond coatings needs to be further studied.

In this work, the preparation and performance tests of HFCVD diamond coatings, deposited on WC-Co samples, are reported. The mechanical properties of single structure diamond coatings were analyzed. A multi-layer coating structure was proposed, based on the advantages of the micro and nano-structured diamond single layers, which would benefit from the properties of the component layers, in order to obtain superior adhesion to the substrate, and improved fracture toughness. Moreover, to evaluate the effectiveness of this multilayer structure, machining tests of natural marble were performed, and the results were compared to those exhibited by the single layer coatings.

Experimental details

Substrate pretreatment

Tungsten carbide 8 mm round samples, with a composition of WC-8%Co (K30, YG8), were used as substrates. The presence of cobalt (Co), used as binder in the tungsten carbide substrate, hinders the nucleation of diamond crystals, instead it induces graphite formation during the deposition process [13]. Consequently, a pretreatment of the substrate plates by acid-etching and alkali treatment was mandatory [14]. This implied the following procedures: (i) Murakami's solution immersion for 10 min, using a solution of potassium ferricyanide and potassium hydroxide (3 g KOH + 3 g $K_3[Fe(CN)_6]$ + 30 ml water), (ii) acid corrosion (3 ml (96%) H_2SO_4 + 60 ml (30%) H_2O_2) [15] for 20 s, (iii) diamond inoculation (the tungsten carbide substrates were dipped into diamond nano-powders with the size of 10 nm in the ultrasonic cleaning machine).

Coating deposition

Diamond coatings were deposited onto cobalt cemented tungsten carbide (YG8) substrate, by hot-filament CVD. The reactor chamber includes a vacuum pump, a cooling system, a gas dosage system, and the power control system. After the pretreatment stages for the substrates and the filaments, the tungsten carbide substrates were placed on the surface of the deposition platform and positioned at 8 mm from the hot filaments. The gas pressure was set at 5.0 KPa and the temperature of hot filament and substrate was 2200 ± 50 °C and 850 ± 30 °C respectively. Other deposition parameters are shown in Table 1. The multi-layer structure of diamond coating has six alternating layers of micro and nanostructured diamond layers. The growth rate of diamond films for MCD and NCD is different according to the concentration of CH_4, and it is also related to the diameter of the filament, size of the reactor chamber, level of seeding, initial surface roughness, among others. According to the concentration of CH_4, the deposition time varied from 6 h to 10.5 h, with the purpose to obtain relatively close film thicknesses between samples.

Table 1
Deposition details of diamond coatings by HFCVD.

Sample number	CH_4 concentration	Deposition time (h)	Gas flow (sccm)	
			CH_4	H_2
1	1%	10.5	8	800
2	3%	7.5	24	800
3	5%	6	40	800
4	1%/5% (Alternate)	8	8/40 (Alternate)	800

Coating analysis

The cross-section morphology of the diamond thin films was detected by field emission scanning electronic microscopy (FESEM), with a HITACHISU-70 microscope, at a testing distance of 8 mm and an applied voltage of 10 kV. In order to assess the surface roughness of the diamond coatings, atomic force microscope (AFM) Innova was used on several test regions of 5 × 5 μm. Five different regions were selected for each diamond coated sample to obtain the average value. The thickness and surface roughness were observed in five different areas with a spacing of 0.5 mm in-between. LabRAM HR was used to obtain the Raman spectra of the diamond coatings, using the laser wavelength of 532 nm and grating of 1800 lines per millimeter. The Raman curves were analyzed by Lorentzian-Gaussian curve-fitting method using a ratio of 80%. The peaks of the crystals are resolved by Lorentz and the amorphous ones by Gaussian. X-ray diffraction patterns for different diamond thin films were obtained using a RINT2000 diffractometer, with Cu-Kα radiation and λ = 0.15406 nm. A Rockwell type hardness tester (LCR500) was used in order to assess the effective adhesive quality of the coatings to the substrate: Rockwell diamond cone with an apex angle of 120° ± 15°, corner radius of 0.02 mm, and 588 N testing load. The tests were carried out on each sample in five different regions, for statistical relevance.

DMG DMU50 milling center was used to evaluate the cutting performance of diamond coated tools. Ball end milling tools with a diameter of 6 mm were used for the machining tests, with the following parameters: a spindle speed of 8000 RPM, a feed speed of 300 mm/min, a radial cutting depth of 0.5 mm and an axial cutting depth of 0.5 mm, all in accordance to the real machining process of natural marble. Kislter 9257B three-dimensional dynamometer was used to detect the cutting force signal. The measurements were carried out every 10 min during the tool life tests and the data acquisition time for each group is 120 s, with a measure frequency of 500 Hz.

Results and discussions

Morphology

The concentration of CH_4 and H_2 has a significant impact on the particle size and crystal form [16]. Fig. 1 shows the SEM pictures of coating-substrate cross-section and morphologies of diamond coatings with different concentrations of CH_4. Considering the morphology of the coatings, i.e. the size and shape of the crystals, the coatings were named: MCD, microcrystalline diamond, NCD – nanocrystalline diamond and ACD – alternate multi-layer crystalline diamond (alternating layers of MCD and NCD-type structures). As Fig. 2 (a) shows, the MCD coating deposited with 1% concentration of CH_4 has a thickness of

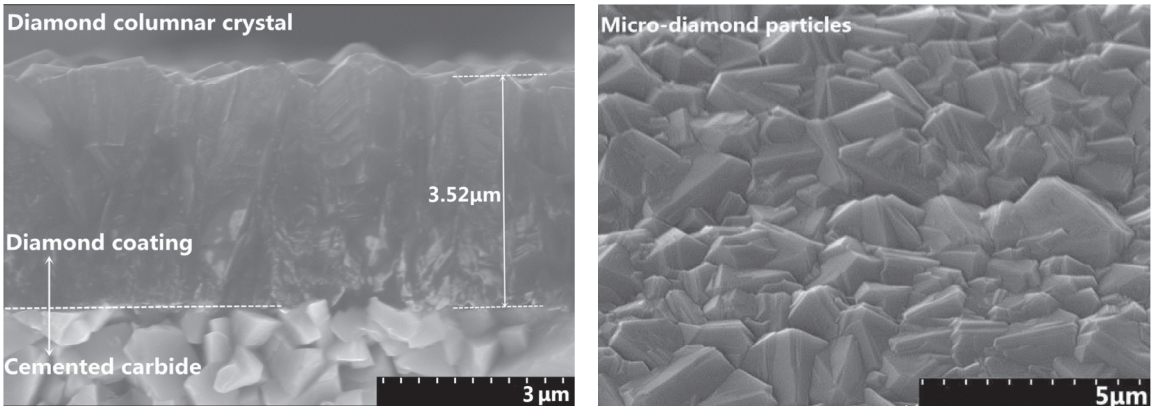

(a) 1% concentration of CH_4

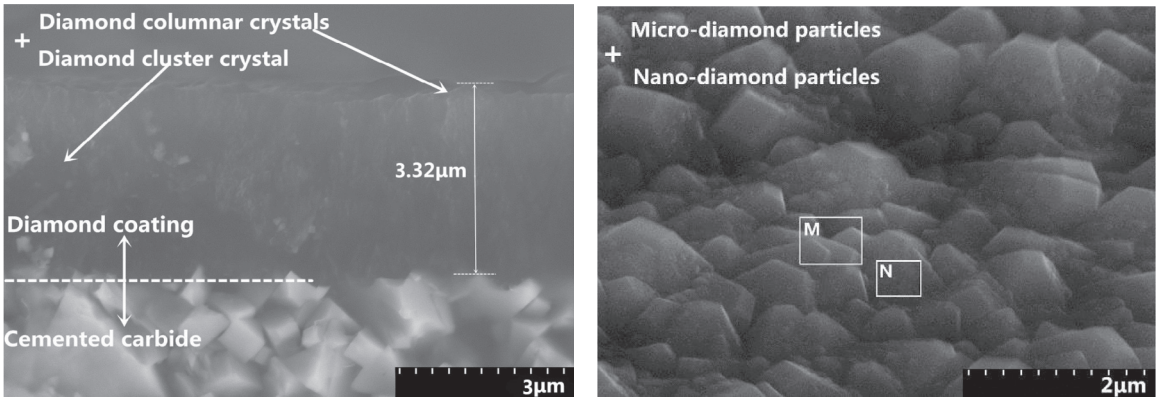

(b) 3% concentration of CH_4

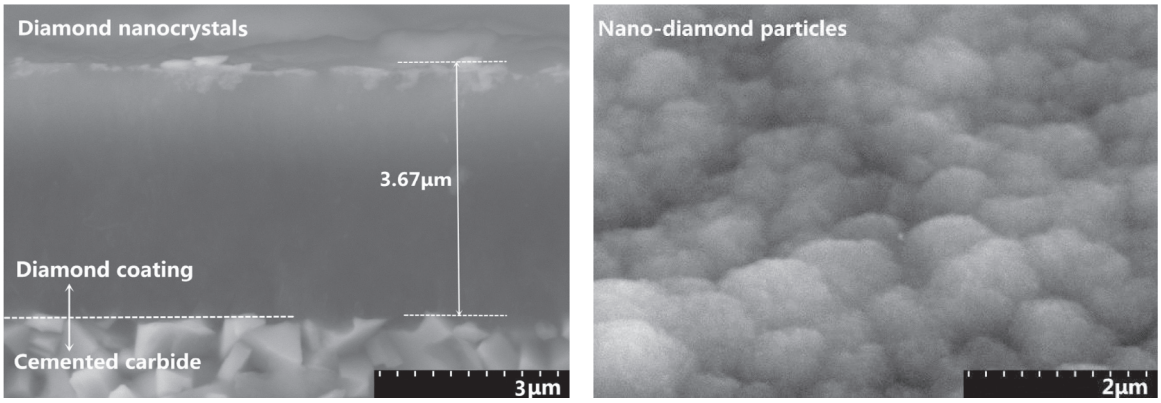

(c) 5% concentration of CH_4

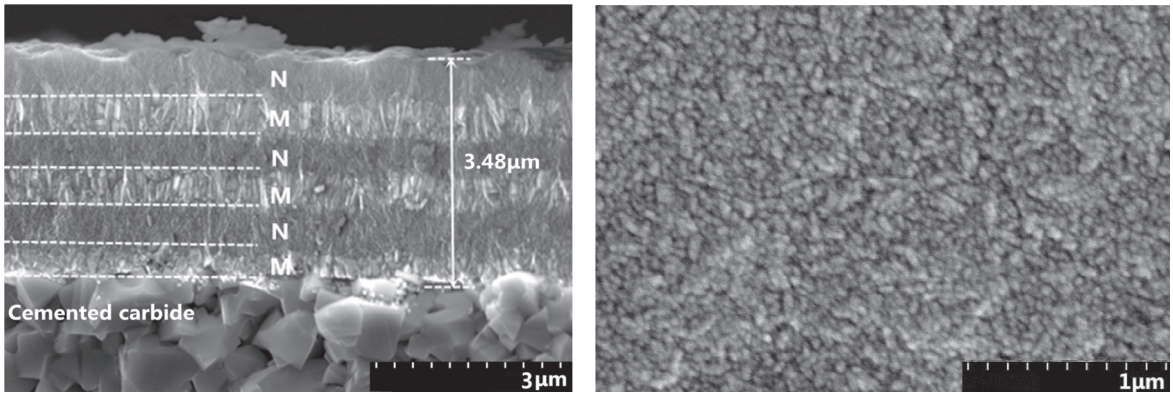

(d) 1% -5% alternate concentration of CH_4

(caption on next page)

Fig. 1. SEM micrographs (cross sections and surface) of HFCVD deposited diamond coatings: (a) 1% concentration of CH_4; (b) 3% concentration of CH_4; (c) 5% concentration of CH_4; (d) 1–5% alternate concentration of CH_4.

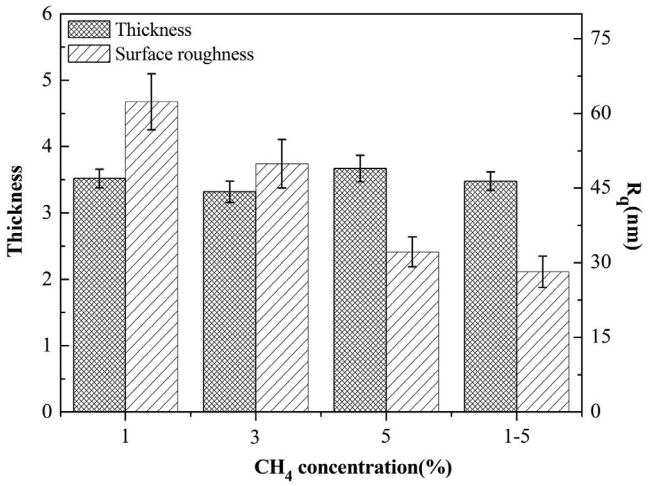

Fig. 2. Thickness and roughness of different diamond coatings.

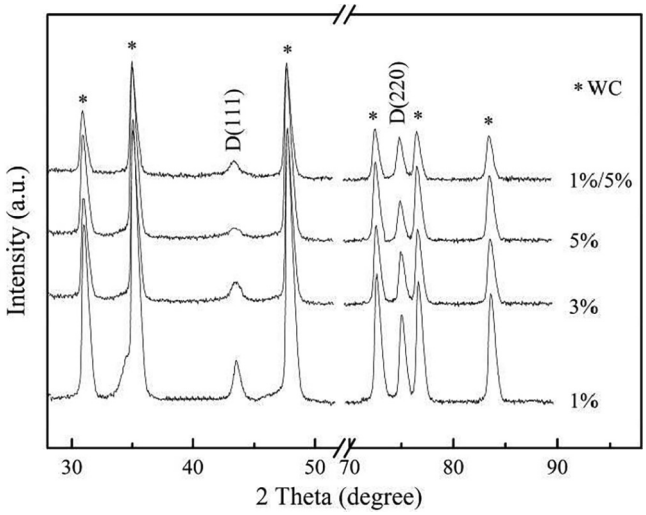

Fig. 3. XRD patterns of CVD diamond coatings deposited with different concentrations of CH_4.

3.52 ± 0.14 μm, the crystals exhibit a typical columnar structure and there is a large contact area at the interface between the coating and the substrate. A strong mechanical anchoring is formed at the interface between the diamond coating and the tungsten carbide substrate. This phenomenon is due to the substrate pretreatment employed before the deposition, which, apart from the cobalt particle removal, significantly increased the surface roughness. Fig. 1(b) shows the section structure morphologies of the diamond coating deposited with 3% concentration of CH_4, where the diamond particles have a size range from 500 nm to 1.2 μm. No certain pattern between the columnar crystals and the nano-clusters was observed. However, the appearance of these nano-clusters is to be noticed. This phenomenon is signifying that the deposition conditions allow for a significantly greater number of nucleation sites, expected from the larger flow of precursor gas. As Fig. 1(c) shows, the diamond columnar crystal structure disappears completely when the concentration of CH_4 is increased to 5%, and the nanometric diamond clusters are predominant. Fig. 1(d) shows the structure of the ACD coating, which exhibits six alternate layers of micro and nano-type structures, deposited with 1% and 5% concentration of CH_4. The micro diamond coating was used as the interface layer between the substrate, while the nanostructured layer was used as the outer layer. Each layer has a thickness of 600 ± 50 nm. According to the results in Fig. 2, the surface roughness decreases from 62.33 nm to 28.18 nm with the increase of CH_4 concentration, which agrees with previous reports on diamond coatings [6]. The main purpose of the specific diamond multilayer structure (ACD) is to obtain higher adhesion strength between the coating and substrate, as well as better fracture toughness, due to multiple interfaces between the individual layers.

Structural analysis (X-ray Diffraction)

Fig. 3 shows the XRD spectra of the samples, deposited with various CH_4 concentrations. The diffraction peak on diamond (1 1 1) plane is located at $2\theta = 43.9^{\circ}$, while the diamond (2 2 0) diffraction peak is located at $2\theta = 75.3^{\circ}$, (PDF 06-675) and the other peaks are tungsten carbide (WC) according to PDF 65-8828. The diffraction peak intensity for both the (1 1 1) and (2 2 0) reflections are decreasing with the increase of CH_4 concentration from 1% to 5%.

Table 2 shows the analysis results obtained from the XRD patterns. The intensity ratio of relative $I_{(2\,2\,0)}/I_{(1\,1\,1)}$ is between 1.11 and 1.51 which is much larger than the corresponding value for a diamond powder 0.25 (25/100, PDF 06-675) which indicates that the diamond

Table 2
Results of XRD patterns of diamond films.

CH_4 concentration (%)	1	3	5	1/5(Alternate)
$I_{(2\,2\,0)}/I_{(1\,1\,1)}$	1.19	1.34	1.51	1.11
FWHM of 111 (°)	0.67	0.92	1.13	0.72
FWHM of 220 (°)	0.65	0.66	0.70	0.71
L_{111} (nm)	12.6	9.16	7.48	11.08
L_{220} (nm)	15.46	15.05	14.19	13.96

coatings deposited in this paper have the preferred growth orientation with the (1 1 0) crystallographic planes [17]. In the case of NCD films, it has been reported that the polycrystalline globular particles are the main formation as the SEM morphology of Fig. 1 shows [16]. The growth mechanism of sphere-like diamond particles is also derived from the appearance of preferential (1 1 0) orientation during diamond films deposition process, according to the preferentially oriented growth mechanism proposed by Silva et al. [18]. The coating deposited with 5% CH_4 concentration exhibits the smallest grain size and higher density of grain boundaries compared to the remaining samples. With the increase of CH_4 concentration, the diamond crystallite size is reduced to 14.19 nm for the sample deposited with 5% CH_4. The crystallinity of the (2 2 0) phase is constant, regardless of the deposition parameters, while there is a decreasing trend for the (1 1 1) phase with the increase of CH_4 concentration. This behavior also indicates that during the transition of MCD to NCD, the (1 1 0) orientation becomes prevalent, which is consistent with the results of $I_{(2\,2\,0)}/I_{(1\,1\,1)}$ ratio. The diamond crystallite size was evaluated using the Scherrer equation [19] (Eq. (1)). The crystallite size (L_{111}, L_{220}) decreased as the CH_4 concentration increased from 1% to 5%, which can be explained due to the high secondary nucleation rate at higher CH_4 concentration conditions, hence the diamond films exhibiting finer crystalline structure and higher grain boundary density, as reported by Gu and Jiang [20].

$$L = \frac{K\lambda}{\beta \cos\theta} \tag{1}$$

where λ is wavelength of X-ray (0.15406 nm), β is the FWHM (full width at half maximum) of diffraction peak and K is a constant value related to crystallite size, usually used as 0.89.

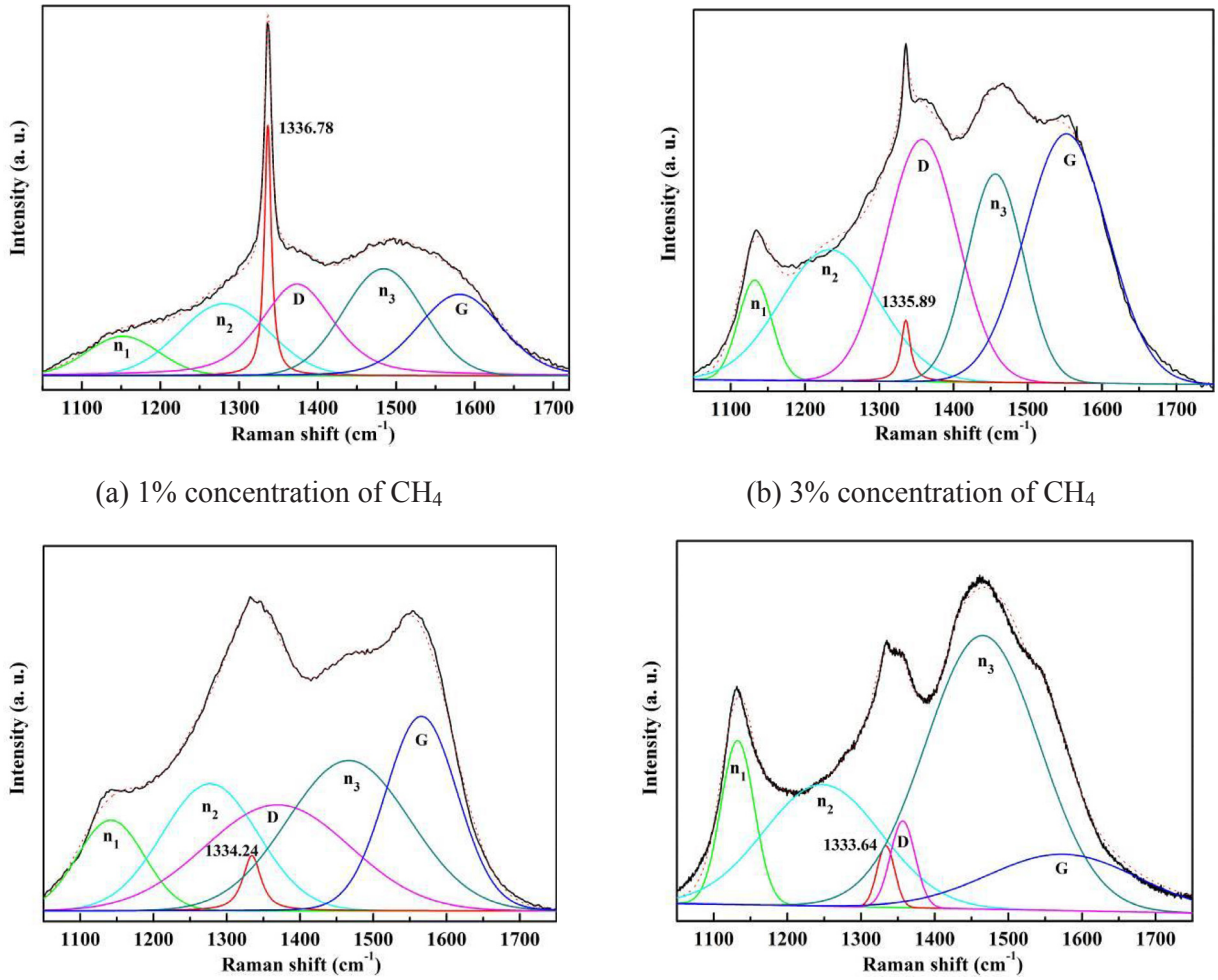

Fig. 4. Raman spectra of CVD diamond coating deposited with different concentrations of CH_4: (a) 1% concentration of CH_4; (b) 3% concentration of CH_4; (c) 5% concentration of CH_4; (d) 1–5% alternate concentration of CH_4.

Raman spectra

The peak deconvolution and attribution from the Raman spectra of coated samples are shown in Fig. 4. The attribution is the following: the peaks situated at n_1 (near 1150 cm^{-1}) and n_3 (near 1450 cm^{-1}) are characteristic for trans-polyacetylene that mainly exist at grain boundaries [21], the peak near n_2 (near 1250 cm^{-1}) is identified as small cluster of diamond, a characteristic peak of diamond sp^3 carbon is present near 1332 cm^{-1}, while the D (disordered) peak (1350 cm^{-1}–1360 cm^{-1}) and G (graphite) peak (1550 cm^{-1}–1580 cm^{-1}) represent carbon with sp^2 bonds [14].

The shift to lower positions for the characteristic peak of diamond sp^3 carbon, as well as the peak intensity, are both decreasing with the increase of CH_4 concentration. In the case of 1% sample, the diamond peak exhibits a higher intensity, compared to the D and G peaks, contrary to the remaining single layer samples. The D and G peaks exhibit an increased intensity, while the diamond peak has a weaker intensity, as the concentration of CH_4 reaches to 3% and 5%, respectively, signifying a shift between the sp^3 and sp^2 bonds. In the case of the ACD coating, the deviation of the diamond peak position decreases even more, to 1333.64 cm^{-1}, while the intensity of the G peak decreases.

Fig. 5 represents the variation of the residual stress (calculated with Eq. (2)) and the FWHM (full width at half maximum), as function of the CH_4 concentration. It can be concluded from Fig. 4 that the FWHM

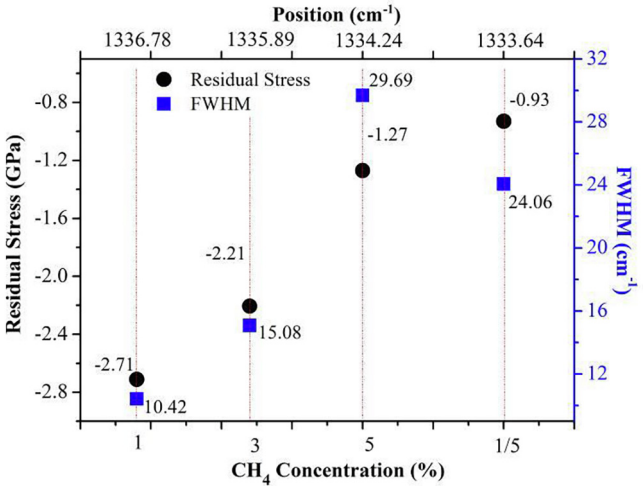

Fig. 5. Residual stress and FWHM of different diamond coated samples.

increases and the diamond crystal quality has a declining trend with the increase of CH_4 concentration. With a higher content of sp^2 carbon, the diamond grains are finer and the density of grain boundaries is larger. The quality of diamond particles decreases with the increase of non-

diamond carbon, observed from the relative intensity of the D and G peaks. As for the ACD coating, the diamond characteristic peak exhibits a lower intensity because the surface layer is composed of material obtained with 5% concentration of CH_4.

Residual stress of the coating can be calculated using the actual peak position value in relation to the standard diamond peak in the Raman spectra, using the following equation [22]:

$$\sigma = -0.567(n - n_0)\ \mathrm{GPa/cm^{-1}} \quad (2)$$

where σ is residual stress, n_0 has a value of 1332 cm^{-1} and v is first-order characteristic peak of diamond in Raman spectrum.

Concerning the single layer diamond coatings, the residual stress (compressive in nature) [23] decreases from −2.71 to −1.27 GPa with the increase of concentration of CH_4 (Fig. 5). The ACD coating has a lower residual stress, down to −0.93 GPa. The influence of thermal stress on the residual stress could be ignored, as the temperature during the deposition was kept at the same value, between depositions.

The residual stress in the diamond coatings is generally related to two aspects: (i) the difference of thermal expansion coefficients between the cemented carbide substrate and the diamond coating, which has a significant effect during the cooling process after high temperature deposition; (ii) intrinsic residual stress derived from non-diamond phases, such as graphite and amorphous carbon. The Raman shift of 1% CH_4 concentration micro-diamond coating is higher than 3% and 5% CH_4 concentration diamond coatings, implying that the residual stress of nano-diamond coating is significantly smaller. Large content of graphite bands indicates the combination of the sp^2 carbon phase at the grain boundaries, on account of smaller particles in nano-diamond coatings according to the diamond crystallite size (Table 2). The large proportion of grain boundaries of amorphous sp^2 carbon leads to the diminishing of crack propagation among inter-crystalline zones, which should lead to better cohesive properties of the diamond films. However, in the ACD coating, the diamond peak located at 1333.2 cm^{-1}, much closer to the standard diamond peak, reflects the significantly decreased internal stress, account for the continuous micro and nano interlocking structure could absorb part of the residual stress as reported by Skordaris et al. [24].

Adhesion analysis

Fig. 6 shows the representative morphology of the diamond coatings after indentation tests. The destructive events can be divided into three types: plastic deformation, radial cracks, and spallation at the edge of the indentation. The spallation of diamond coatings occurs under the external forces around the indenter in a relatively small area, for all samples, as Fig. 6(a) shows. As the 1% sample is concerned, within the circumferential range of 277 ± 25 μm, the diamond coating concaved downward. The initial cracks extend outward from the interior of micro-diamond through the inter-granular diffusion. The adhesion strength of the micro diamond structure (sample 1%) is relatively acceptable and the spallation of the coating cannot occur easily, considering the relatively low spalled area. However, the resistance to crack propagation is significantly poorer, compared to the remaining samples, mostly due to the inability of the columnar crystal structure to accommodate this aspect. The adhesion behavior of MCD and NCD films is consistent with the results obtained through scratch tests by Dumpala et al. [25], the MCD shows a better interface binding strength and worse resistance to crack propagation compared with NCD films.

As the concentration of CH_4 increases, the adhesion strength decreases (the spalled surface area is significantly larger for samples 3% and 5%), however the crack propagation area is reduced. The crack propagation area in Fig. 6(b) has a circle radius of 198 ± 15 μm around the indenter center, which is smaller than the indentation results of the 1% sample. The internal crack expansion area decreases, and the coating spallation is aggravated for the nano-diamond structure, as Fig. 6(c) shows. Due to large structure density of cluster diamond combination, the resistance ability of NCD coating to inter-crack propagation is better than MCD coating. For the multi-layer film, the columnar layer is used as the interface between the substrate and the first NCD layer, to obtain better adhesion to the substrate, while the nano-diamond structure was used as the surface layer. There is no obvious crack propagation area around the center of the indenter imprint, according to the micrograph (Fig. 6(d)). Moreover, the nano-diamond particles have lower surface roughness, an aspect which is critical if these coatings should be used for high-precision machining tools.

Machining performance

To investigate the machining characteristics of different kinds of diamond coated tools, up milling experiments (as Fig. 7 shows) of CVD diamond coated cobalt cemented tungsten carbide milling tools were made. The tool tracks keep in the same milling direction as Fig. 7 shows. The milling tools were prepared with the same substrate material and deposition parameters as the flat samples, presented in the previous sections.

The workpiece for cutting was natural marble, with a dimension of 200 × 300 × 15 mm, the physical characteristics shown in Table 3. The wear area was observed by SEM every 10 min after machining. The surface roughness of machined workpiece was measured by Tylor-Hobson Roughness Tester. The end of tool life criterion was 250 μm of flank wear and each wear width was observed in 5 different regions of flank face and averaged.

Fig. 8 shows the service life of cutting tools, uncoated and coated tools with CH_4 concentration of 1%, 3%, 5%, alternate 1%/5%. It can be seen there is a significant improvement for the tool life of the ACD coating, compared with the uncoated and the single layer coated tools. A rapid failure process of uncoated WC-Co tool shows up within 30 min. The nano diamond (5%) coated tool exhibits almost a linear growth regarding the wear capacity, with a tool life of 40 min. As for the diamond coated tool with the CH_4 concentration of 3%, a similar, albeit slightly better behavior is shown, with a service life increased to 80 min. The run-in process of 1% CH_4 concentration diamond coated tool has a period OA of 30 min and the stable period AD continued for 50 min. There is a longer run-in period OB of ACD coated tool which lasts 50 min, the wearing capacity after the initial machining process showing a steady increasing trend. The stable cutting process lasts 60 min and the whole effective machining period has a 150-minutes running time. The service life and machining stability of cutting tools were effectively improved by the ACD coating. Fig. 9 exhibits the mean value during the whole machining period of different tools. The ACD coated tool produced the best Ra of machined workpiece, 1.7 μm and the uncoated one is the poorest one with the value of 3.5 μm.

Fig. 10 shows the relationship between flank face wearing capacity/cutting forces and surface roughness of workpiece milled with ACD coated tools. The nano-diamond layer deposited with 5% concentration of CH_4 was used for the external surface of coated tools, because it has a smaller value of surface roughness which leads to better machined surface quality. During the initial cutting period, the surface roughness changes in the range of 0.42–1.0 μm. The cutting forces from three directions are influenced by flank face wearing capacity. According to the curves in Fig. 10, a large number of acquisition points concentrate on the steady wear region of machining, and the value of V_B changes in a small range, therefore, the cutting performance of alternate multi-layer diamond coated machining tool is stable during the effective service life. The average values of cutting forces of different tools used in the tests during different machining period were shown in Fig. 10. The values of T1, T2 and T3 represent the cutting force at the beginning, mid and end of the tool life, respectively. ACD coated tool exhibits the lowest values, especially during the mid-period, which signifies stable machining performance. Comparing the forces, they are increasing with the rise of the roughness of tool surface (see Fig. 11).

Fig. 12(a) exhibits the SEM images of uncoated tool after

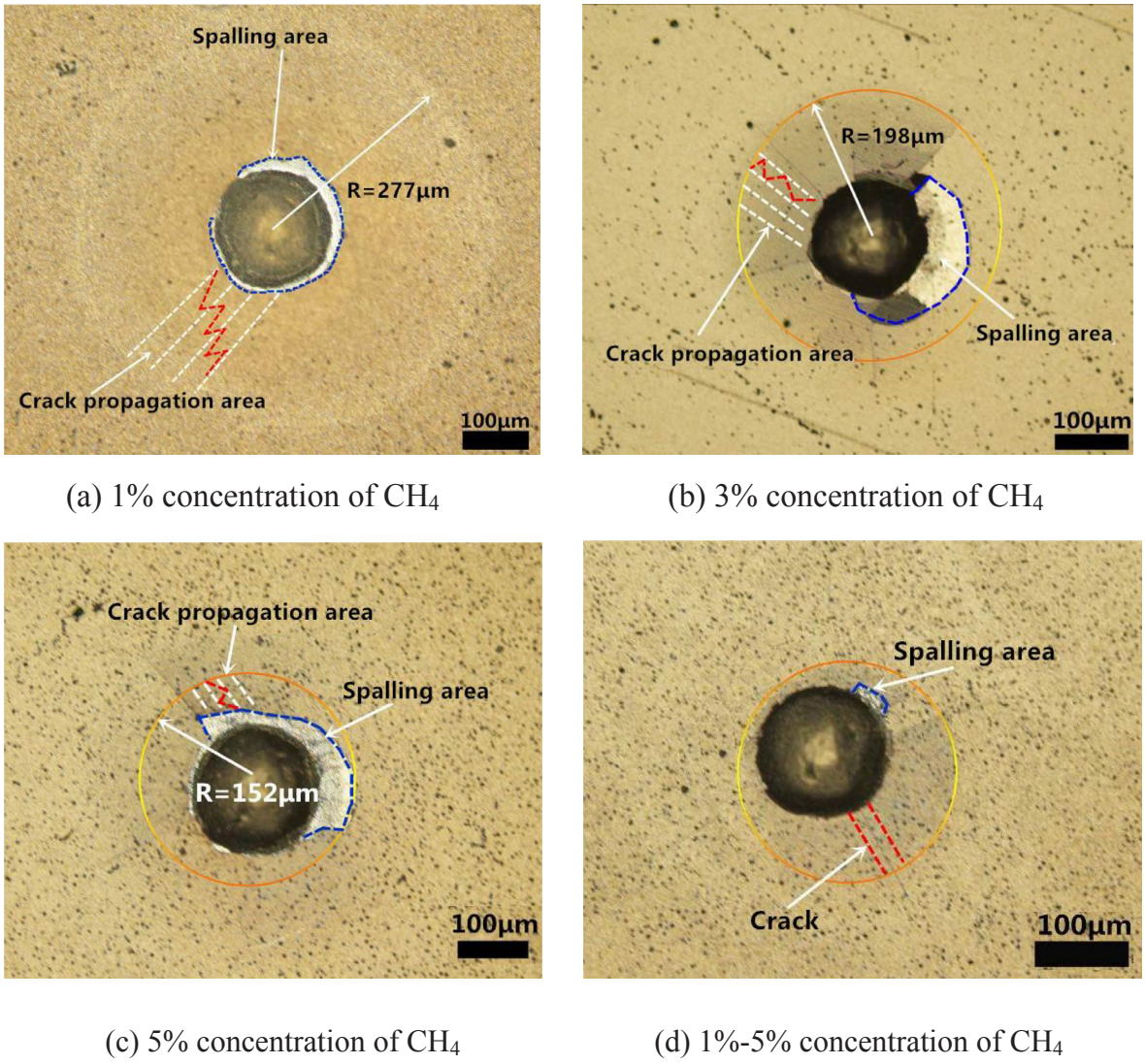

Fig. 6. Micrographs of the Rockwell C indentations with a load of 588N on diamond coated WC-Co substrate with different structures: (a) 1% concentration of CH_4; (b) 3% concentration of CH_4; (c) 5% concentration of CH_4; (d) 1–5% alternate concentration of CH_4.

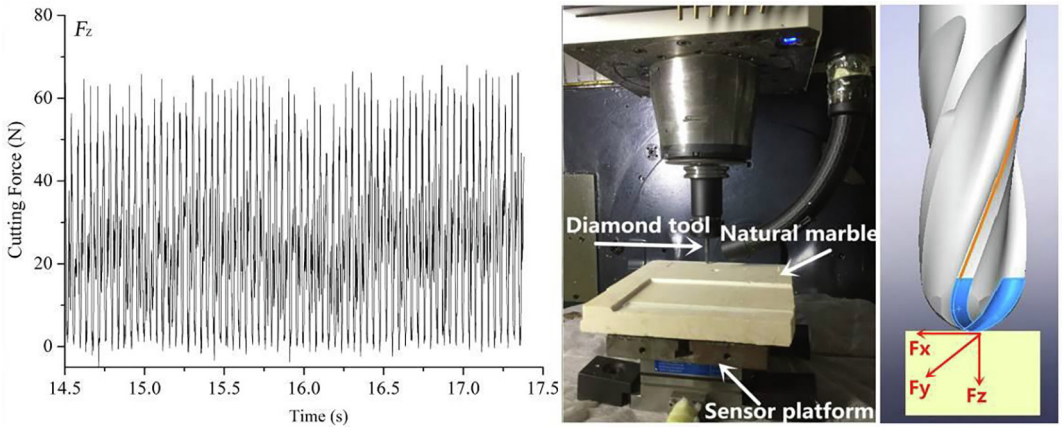

Fig. 7. Machining system of natural marble milled by CVD diamond coated tools.

machining. The integrity of the cutting edge was destroyed under the intermittent impact stress. The marble powder attached to the surface of the cutting edge and decreased the machining ability of the milling tool. Fig. 12(b) shows the wear morphology of micro-diamond coated tool, deposited with 1% concentration of CH_4, after milling for 120 min. The resistance to crack propagation of the micro columnar structure is reduced, the initial cracks seem to diffuse along the inter-crystalline regions, and then through-thickness cracks appear. With the progress of the machining process, the diffusion of cracks leads to inter-crystalline fracture inside the diamond coating, and spallation of the diamond

Table 3
Physical properties of natural marble [26].

Properties	Density (kg/m^3)	Water absorption (%)	Compressive strength (MPa)	Abrasion resistance index	Shock strength (cm)	Elasticity modulus (MPa)	Mohs hardness
White marble	2705	0.24	92	0.52	61	75,000	3.5

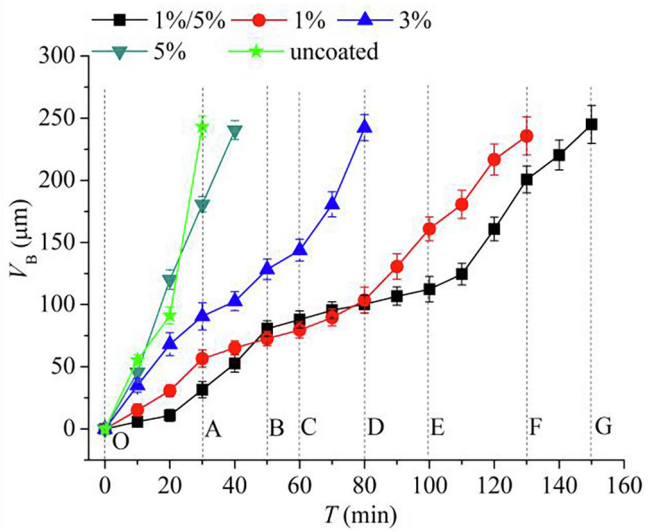

Fig. 8. Wear width of flank face as a function of machining time.

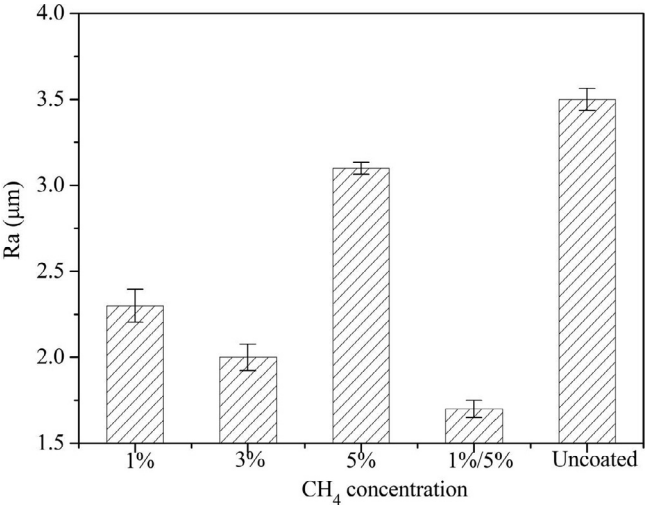

Fig. 9. Workpiece surface roughness of different tools.

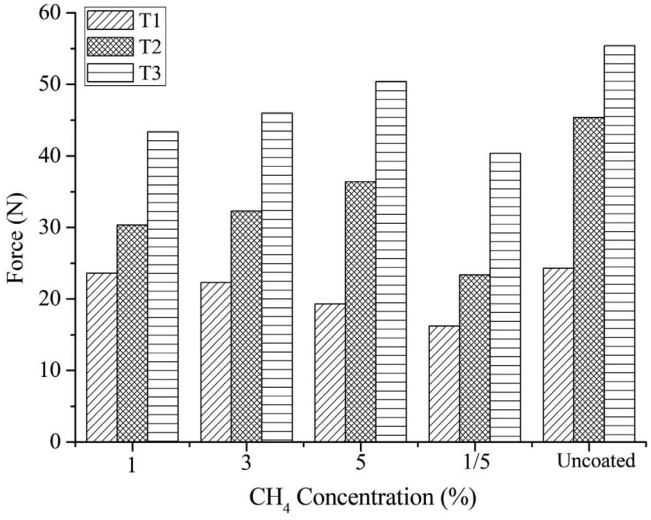

Fig. 10. Average force of different tools at the beginning, mid and end of the tool life.

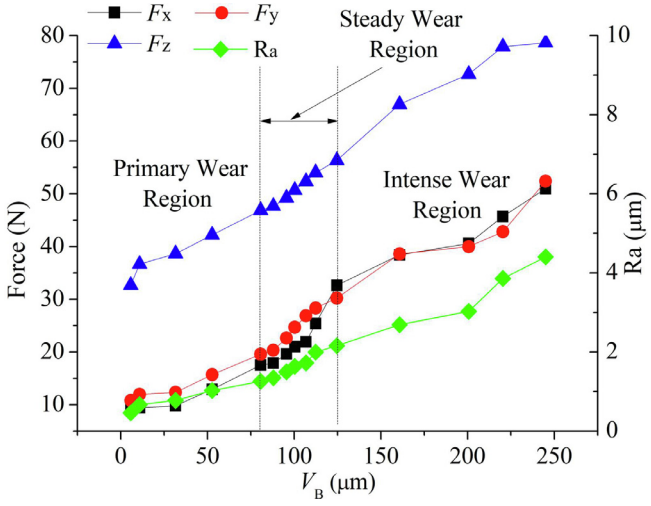

Fig. 11. Cutting force and workpiece surface roughness as a function of flank face wear width.

coating from the substrate occurs.

As Fig. 12(c) and (d) show, the expansion for the initial cracks is noticed, for the samples deposited with the 3% and 5% concentration of CH_4 respectively, related to the effect of high residual stress inside the material. It was shown in the previous sections that the nano-diamond samples exhibit weak adhesion strength between the coating and the substrate. This effect is noticed on the milling tools as well, the coatings peeling off from a large area under the influence of cycling stress in the machining process.

The wear area of the ACD multi-layer diamond coated tool after milling is significantly smaller than the single-layer diamond samples, to the point where it reaches the standard width of blank face wear extent, as Fig. 12(e) shows. The structural advantages of the micro and nano coatings, i.e. better adhesion strength and improved crack resistance ability seem to contribute to a significantly better wear performance during milling.

Conclusions

(1) Diamond coatings with the CH_4 concentrations of 1%, 3%, 5% and alternate 1%/5% were deposited on WC-Co substrate by HFCVD. The adhesion strength of the micro columnar structure diamond coating is better than the nano-cluster diamond structure coatings. The nanocrystalline cluster diamond structure exhibits higher nucleation density which leads to better ability to prevent internal crack propagation. The ACD film (alternate multi-layer crystalline diamond) integrates several desired properties, necessary for the application of cyclic milling of hard/brittle materials: reduced surface roughness; resistance to internal crack propagation,

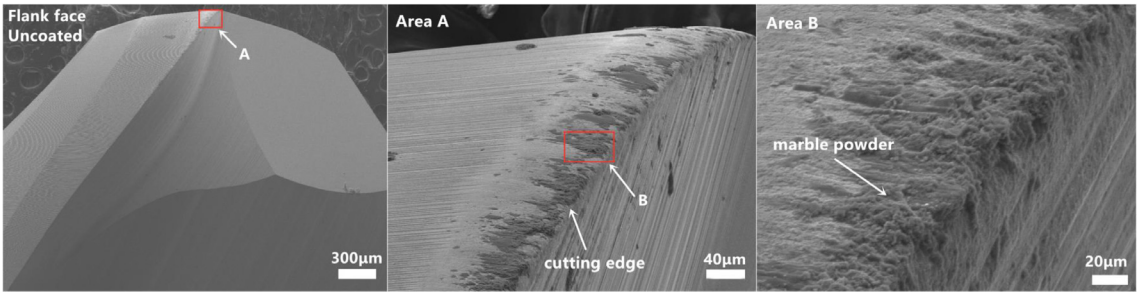

(a) Uncoated tool

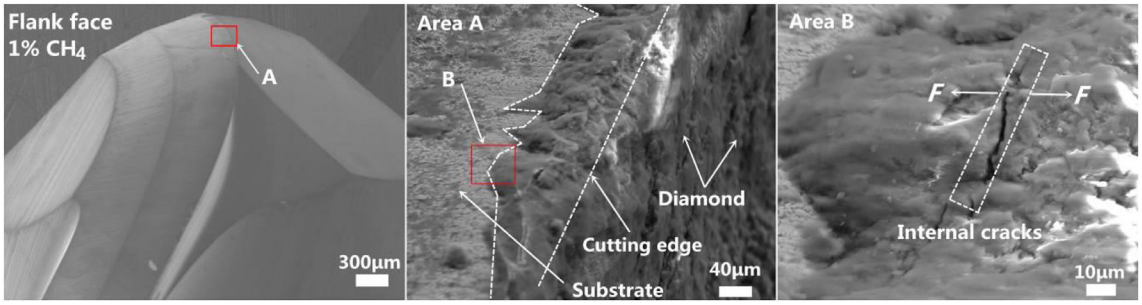

(b) 1% CH_4 coated tool

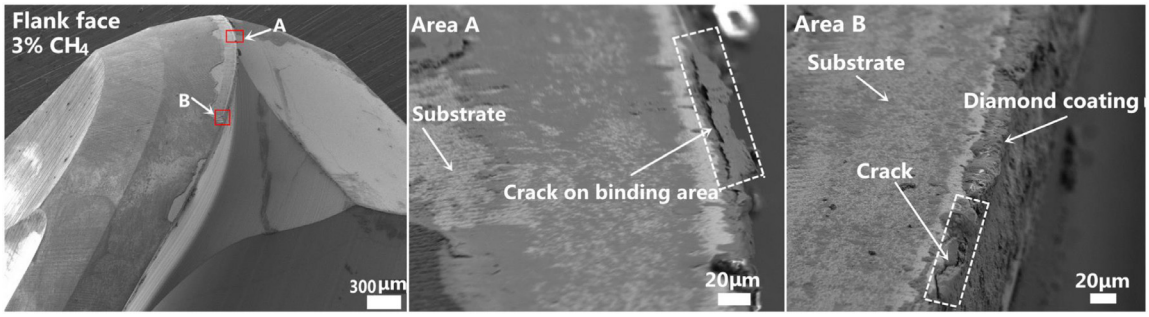

(c) 3% CH_4 coated tool

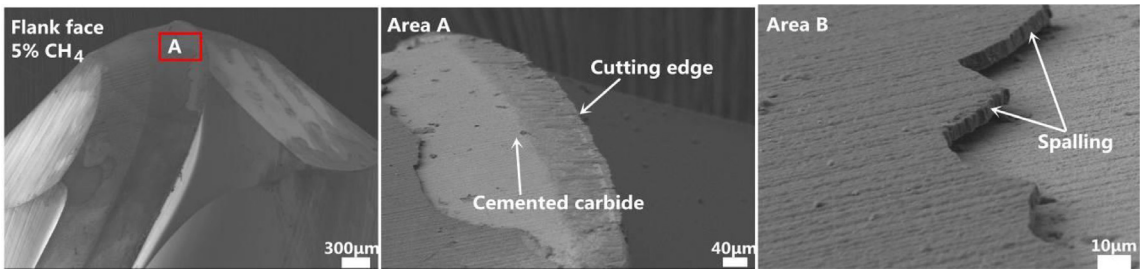

(d) 5% CH_4 coated tool

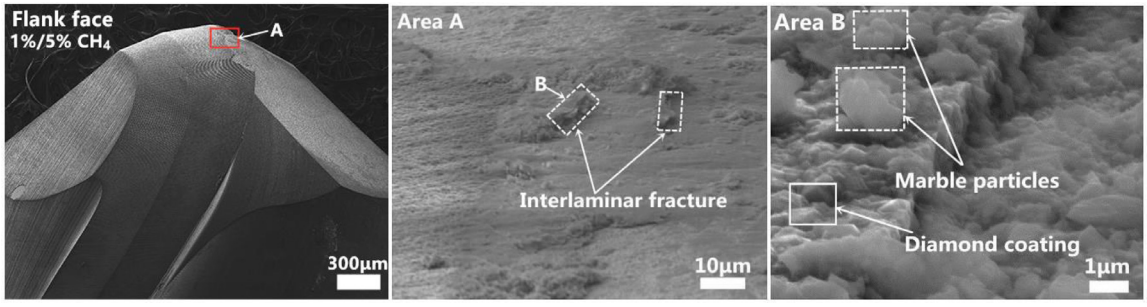

(e) 1%/5% CH_4 coated tool

(caption on next page)

Fig. 12. SEM wear morphology of diamond coated tools deposited with different parameters, after machining: (a) uncoated tool; (b) 1% CH_4 coated tool; (c) 3% CH_4 coated tool; (d) 5% CH_4 coated tool; (e) 1–5% alternate CH_4 coated tool.

conferred by the nano-diamond layers; the high adhesion strength, conferred by the micro diamond interface layer.

(2) The results of cutting experiments of different tools indicate that the service life and machining quality of ACD coated machining tool is significantly superior to other single layer and uncoated tools. The main failure mode of nano-diamond coated tool is focused on the film delamination from the substrate, which derives from the significant internal stress. As for the micro-diamond coated tools, the diffusion of internal cracks leads to coating failure. The surface quality of the workpiece (natural marble) and machinability of the ACD coated tool suggest reliability and practicality for the real machining process of hard-brittle materials.

Acknowledgements

This research is sponsored by Natural Science Foundation of Liaoning Province, China (20170540757), Scientific and Technological Transformative Project of Shenyang (Z18-5-023, Z17-0-027 and Z18-0-025).

References

[1] Hu G, Fang FZ, Hu XT. Kinematic view of tool life in rotary ultrasonic side milling of hard and brittle materials. Int J Mach Tools Manuf 2010;50(3):303–7.
[2] Liu JW, Baek DK, Ko TJ. Chipping minimization in drilling ceramic materials with rotary ultrasonic machining. Int J Adv Manuf Technol 2014;72(9–12):1527–35.
[3] Sein H, Ahmed W, Jackson M, Woodwards R, Polini R. Performance and characterisation of CVD diamond coated, sintered diamond and WC–Co cutting tools for dental and micromachining applications. Thin Solid Films 2004;447:455–61.
[4] Polini R. Chemically vapour deposited diamond coatings on cemented tungsten carbides: substrate pretreatments, adhesion and cutting performance. Thin Solid Films 2006;515(1):4–13.
[5] Almeida FA, Sacramento J, Oliveira FJ, Silva RF. Micro-and nano-crystalline CVD diamond coated tools in the turning of EDM graphite. Surf Coat Technol 2008;203(3–4):271–6.
[6] Ali M, Ürgen M. Surface morphology, growth rate and quality of diamond films synthesized in hot filament CVD system under various methane concentrations. Appl Surf Sci 2011;257(20):8420–6.
[7] Sarangi SK, Chattopadhyay A, Chattopadhyay AK. Influence of process parameters on growth of diamond crystal on cemented carbide substrates by HFCVD system. Int J Refract Metal Hard Mater 2012;31:1–13.
[8] Dumpala R, Kumar N, Kumaran CR, Dash S, Ramamoorthy B, Rao MR. Adhesion characteristics of nano-and micro-crystalline diamond coatings: Raman stress mapping of the scratch tracks. Diam Relat Mater 2014;44:71–7.
[9] Qin F, Hu J, Chou YK, Thompson RG. Delamination wear of nano-diamond coated cutting tools in composite machining. Wear 2009;267(5–8):991–5.
[10] Khomich AV, Kozlova MV, Ashkinazi EE, Sedov VS, Sovyk DN, Vinogradov DV, Tsygankov PA. Microwave CVD deposition and properties of nano/microcrystalline diamond multilayer coatings on tungsten carbide cutting tools. In: 2017 International Conference on Mechanical, System and Control Engineering (ICMSC). IEEE; 2017. p. 11–15.
[11] Sun FH, Zhang ZM, Chen M, Shen HS. Fabrication and application of high-quality diamond-coated tools. J Mater Process Technol 2002;129(1–3):435–40.
[12] Wang C, Wang X, Sun F. Tribological behavior and cutting performance of monolayer, bilayer and multilayer diamond coated milling tools in machining of zirconia ceramics. Surf Coat Technol 2018;353:49–57.
[13] Klauser F, Steinmüller-Nethl D, Kaindl R, Bertel E, Memmel N. Raman studies of nano-and ultra-nanocrystalline diamond films grown by hot-filament CVD. Chem Vap Depos 2010;16(4–6):127–35.
[14] Ferrari AC, Robertson J. Raman spectroscopy of amorphous, nanostructured, diamond–like carbon, and nanodiamond. Philos Trans Roy Soc Lond A: Math Phys Eng Sci 1824;2004(362):2477–512.
[15] Wei Q, Yu ZM, Ashfold MN, Ye J, Ma L. Synthesis of micro-or nano-crystalline diamond films on WC-Co substrates with various pretreatments by hot filament chemical vapor deposition. Appl Surf Sci 2010;256(13):4357–64.
[16] Yang TS, Lai JY, Cheng CL, Wong MS. Growth of faceted, ballas-like and nanocrystalline diamond films deposited in $CH_4/H_2/Ar$ MPCVD. Diam Relat Mater 2001;10(12):2161–6.
[17] Kobashi K, Nishimura K, Miyata K, Kumagai K, Nakaue A. (110)-oriented diamond films synthesized by microwave chemical-vapor deposition. J Mater Res 1990;5(11):2469–82.
[18] Silva F, Bénédic F, Bruno P, Gicquel A. Formation of < 110 > texture during nanocrystalline diamond growth: an X-ray diffraction study. Diam Relat Mater 2005;14(3–7):398–403.
[19] Scherrer P. Bestimmung der Grösse und der Inneren Struktur von Kolloidteilchen Mittels Röntgenstrahlen, Nachrichten von der Gesellschaft der Wissenschaften, Göttingen. Mathematisch-Physikalische Klasse 1918;2:98–100.
[20] Gu CZ, Jiang X. Deposition and characterization of nanocrystalline diamond films prepared by ion bombardment-assisted method. J Appl Phys 2000;88(4):1788–93.
[21] Pfeiffer R, Kuzmany H, Knoll P, Bokova S, Salk N, Gunther B. Evidence for transpolyacetylene in nano-crystalline diamond films. Diam Relat Mater 2003;12(3–7):268–71.
[22] Fan QH, Gracio J, Pereira E. Evaluation of residual stresses in chemical-vapor-deposited diamond films. J Appl Phys 2000;87(6):2880–4.
[23] Roy M, George VC, Dua AK, Raj P, Schulze S, Tenne DA, et al. Feed gas dependence of the surface nanophase on HFCVD grown diamond films studied by surface enhanced Raman spectroscopy. Appl Surf Sci 2002;191(1):334–7.
[24] Skordaris G, Bouzakis KD, Charalampous P, Kotsanis T, Bouzakis E, Lemmer O. Effect of structure and residual stresses of diamond coated cemented carbide tools on the film adhesion and developed wear mechanisms in milling [J]. Cirp Ann-Manuf Techn 2016;65(1):101.
[25] Dumpala R, Chandran M, Kumar N, Dash S, Ramamoorthy B, Rao MR. Growth and characterization of integrated nano-and microcrystalline dual layer composite diamond coatings on WC–Co substrates. Int J Refract Metal Hard Mater 2013;37:127–33.
[26] Carmichael RS. Practical handbook of physical properties of rocks and minerals (1988) [M]. CRC Press; 2017.